

imdea
materiales

A ROADMAP FOR VIRTUAL TESTING AND VIRTUAL PROCESSING OF CAST METALLIC MATERIALS

Javier LLorca

IMDEA Materials Institute & Polytechnic University of Madrid

*2nd Int. Workshop on Software Solutions for Integrated Computational Materials Engineering
Barcelona, 12th-15th, April, 2016*

1. MOTIVATION

- Integrated Computational Materials Engineering
- Virtual design of cast metallic components

2. Virtual processing of Ni-based superalloys

3. Virtual testing of Ni-based superalloys

4. Conclusions

Objective

● Virtual design, virtual processing and virtual testing of new materials *in silico*, before they are actually manufactured in the laboratory.

Benefits

- Accelerate materials development (reduce time to market).
- Integrate materials into the design optimization process.
- Unify design and manufacturing.

Strategy

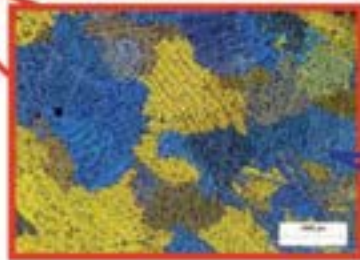
● Integration of all available modeling tools into a multiscale strategy capable of simulating processing, structure, properties and performance of engineering materials.

What is the worst scenario for ICME?

cast Al alloys (J. E. Allison, JOM, 2006)



**1 m
Engine Block**



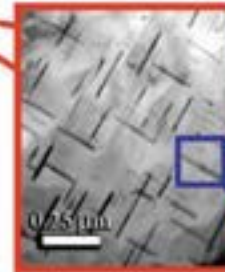
**1–10 mm
Macrostructure**

- Grains
- Macroporosity
- Properties**
- High-cycle fatigue
- Ductility



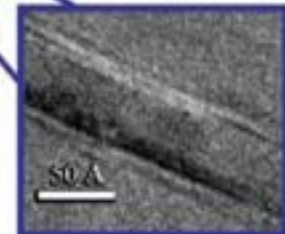
**10–500 μm
Microstructure**

- Eutectic Phases
- Dendrites
- Microporosity
- Intermetallics
- Properties**
- Yield strength
- Tensile strength
- High-cycle fatigue
- Low-cycle fatigue
- Thermal Growth
- Ductility




**1–100 nm
Nanostructure**

- Precipitates
- Properties**
- Yield strength
- Thermal Growth
- Tensile strength
- Low-cycle fatigue
- Ductility

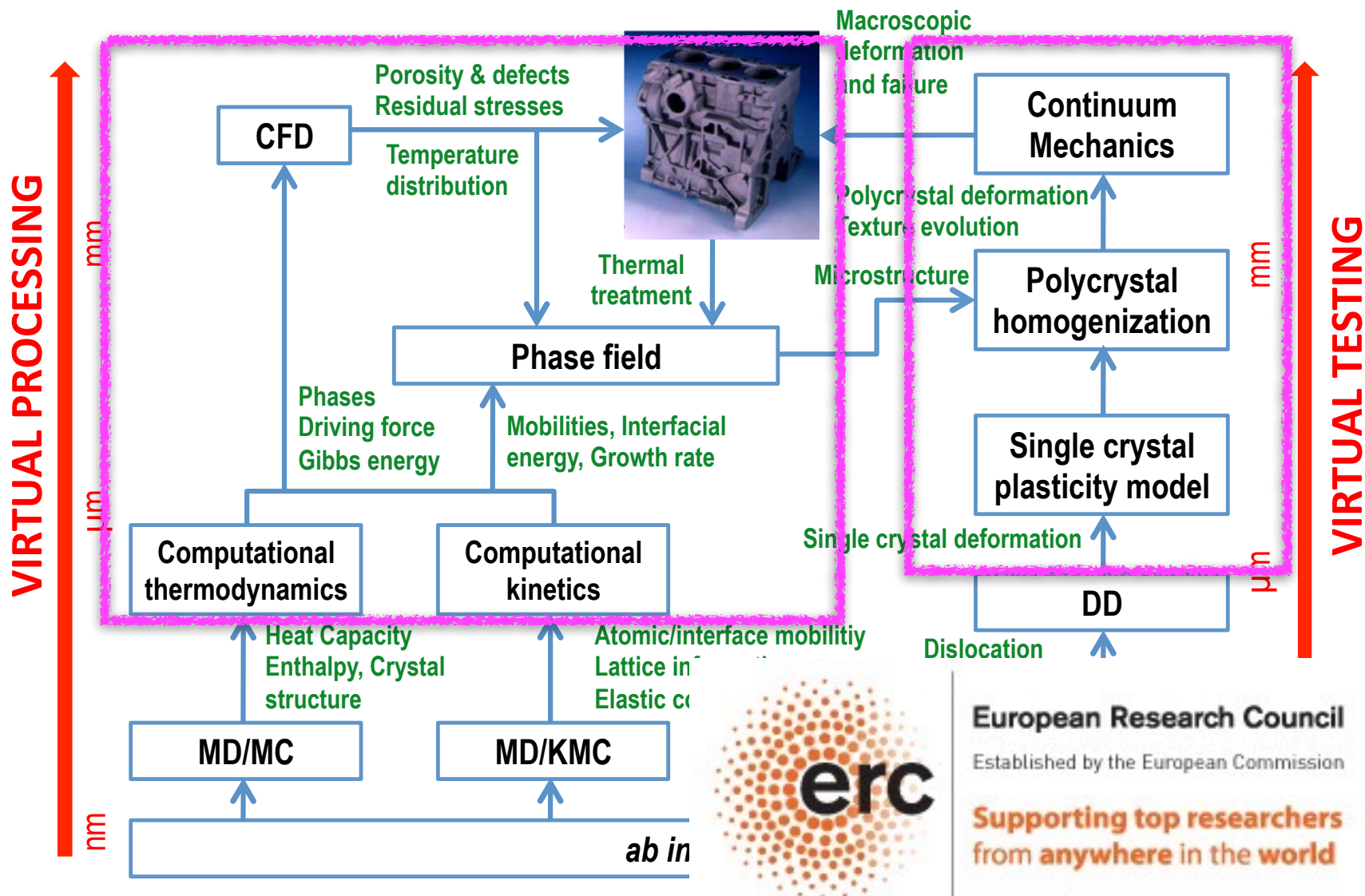


**0.1–1 nm
Atomic Structure**

- Crystal Structure
- Interface Structure
- Properties**
- Thermal Growth
- Yield Strength

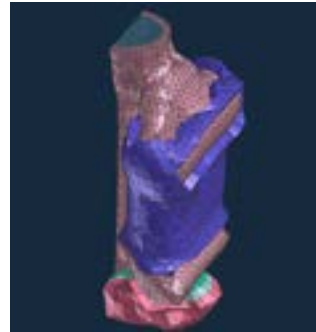
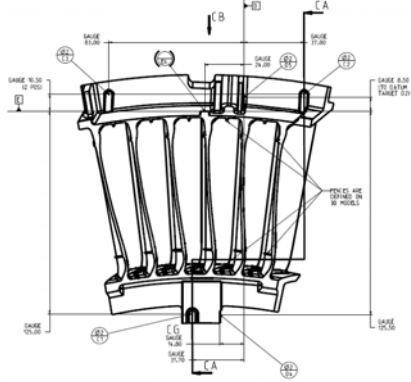
 Mechanical properties of cast metals (stiffness, strength, toughness, fatigue limit) depend on phenomena and structures that span over 9 orders of magnitude!

VIRTUAL DESIGN



VIRTUAL CASTING OF ENGINEERING ALLOYS

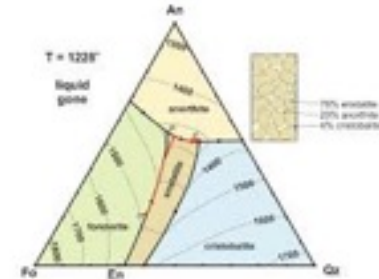
Component design



component & wrapping

Geometry

Solidification



computational thermodynamics

Mold filling & solidification simulation


Thermal

Validation

Porosity
Grain size

Casting experiments




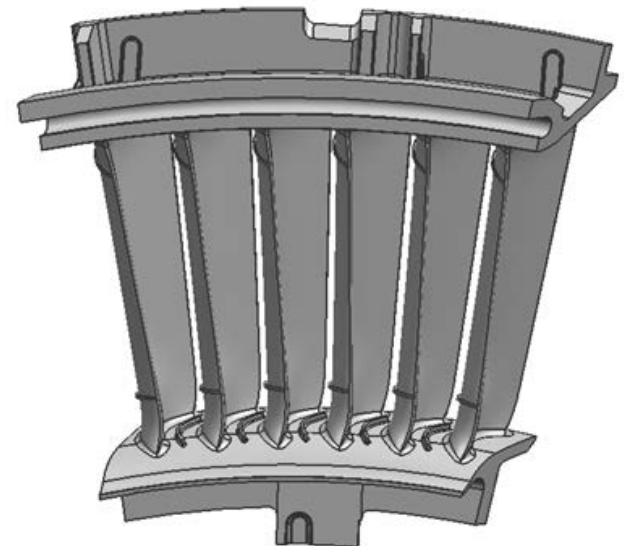
 MAR 247 is a polycrystalline Ni-based superalloy with outstanding mechanical properties at high temperature due to the W, Hf and Ta content, which is widely used in nozzle guide vanes, blades and disks in gas turbines.


Chemical composition

Element	Ni	W	Cr	Mo	Co	Al	Ti	C	Hf	Ta
Weight (%)	balance	10	8.4	0.7	10	5.5	1.05	0.15	1.4	3.1

COMPONENT

 Nozzle guide vane for a gas turbine with complex shape and thinner wall sections to be manufactured by investment casting designed by ITP.

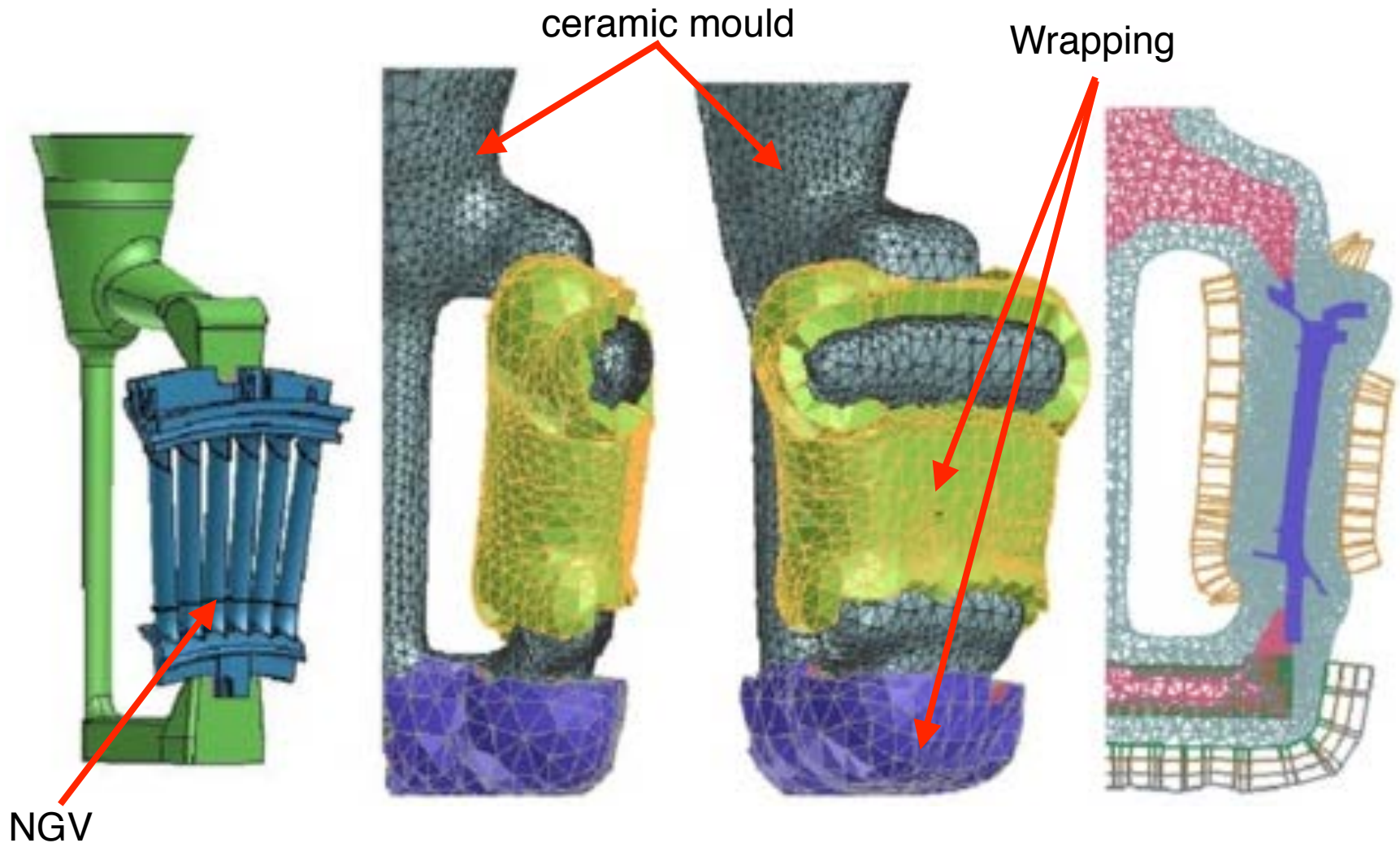


 Accurate prediction of the temperature profile in the cast during solidification is critical. This is a very difficult task because of the **different heat transfer mechanisms** (radiation, conduction, convection) and the **different materials** involved (metal, mould shell and insulation wrap), together with the corresponding interfaces.




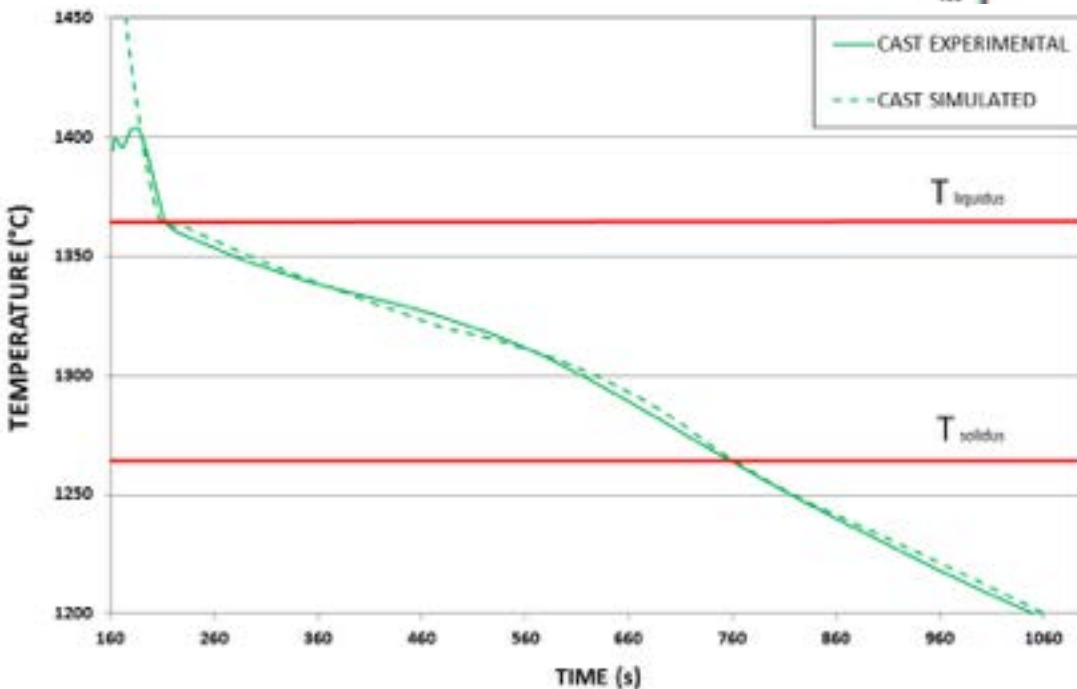
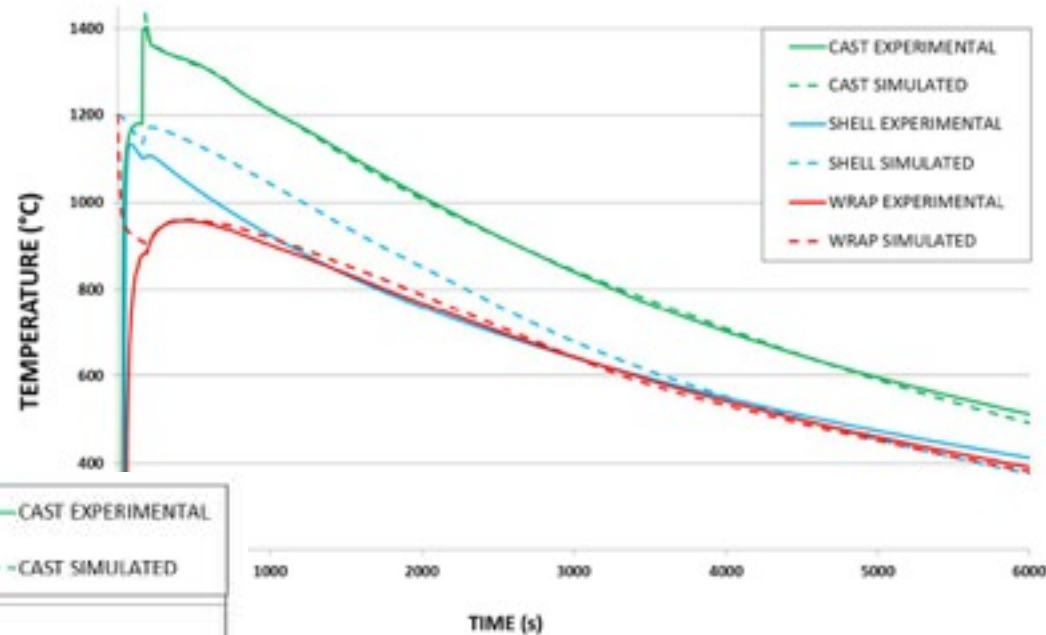
THERMAL MODEL

Finite element model of the NGV, mould and wrapping.

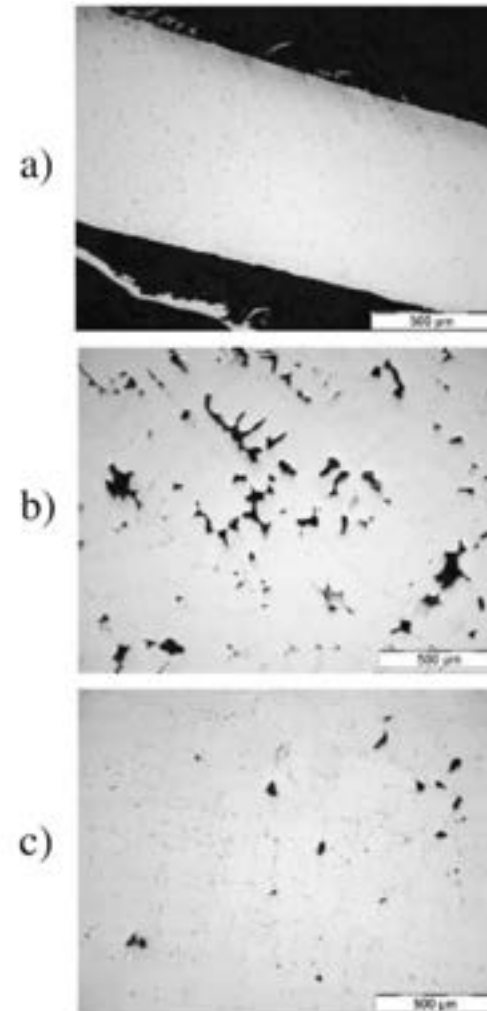
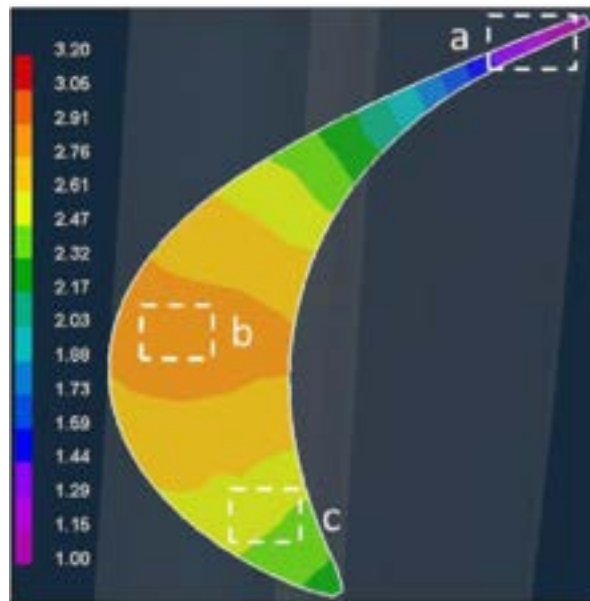


THERMAL MODEL

 The thermal properties of the different materials and interfaces were fitted from the experimental temperatures measured in the casting experiments.



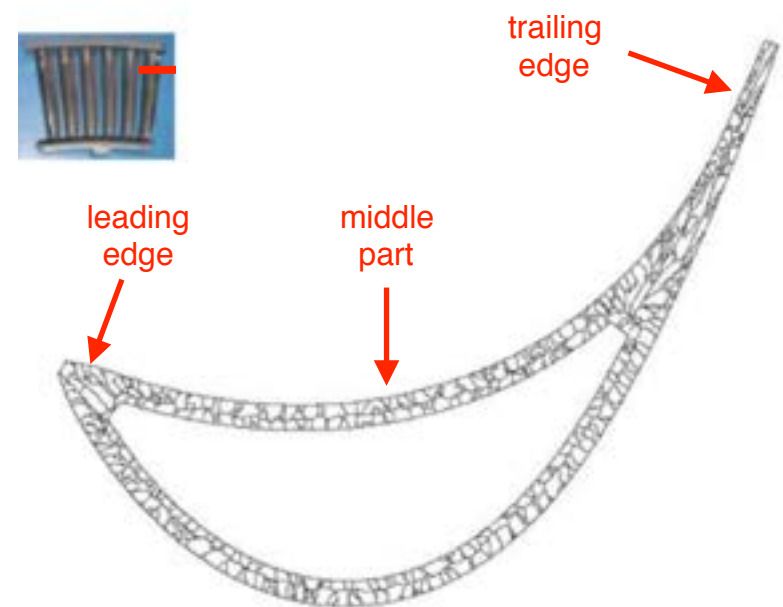
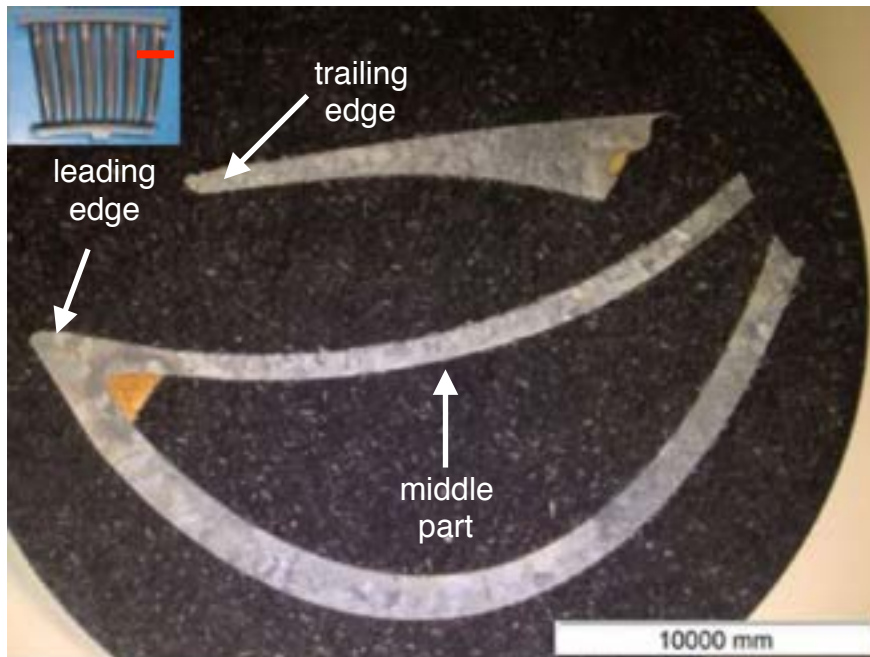
Shrinkage porosity and microporosity were computed by taking into account the progress of solid, mushy and liquid regions in the cast during solidification.



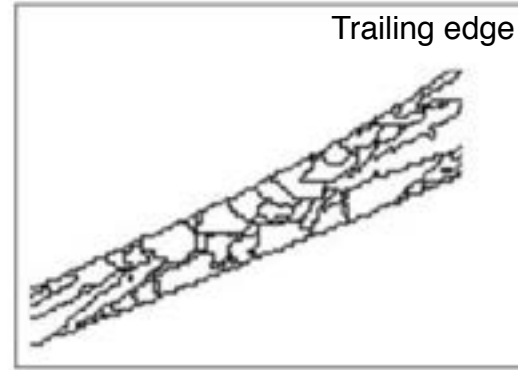
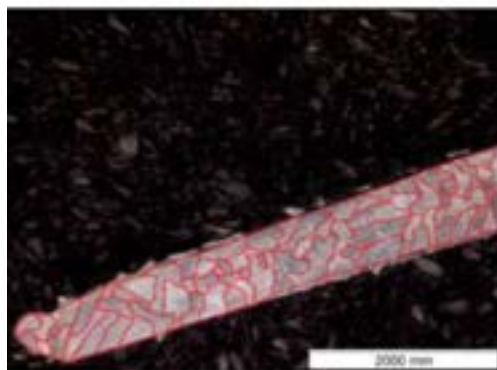
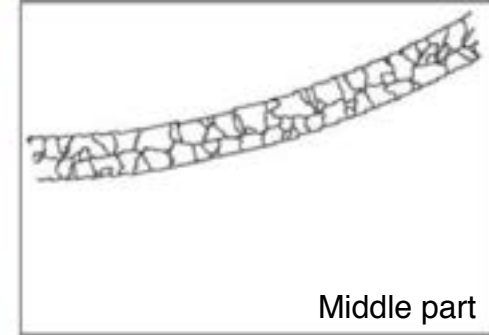
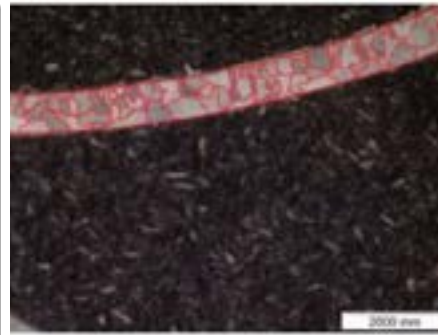
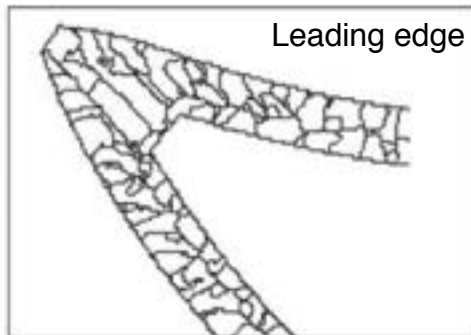
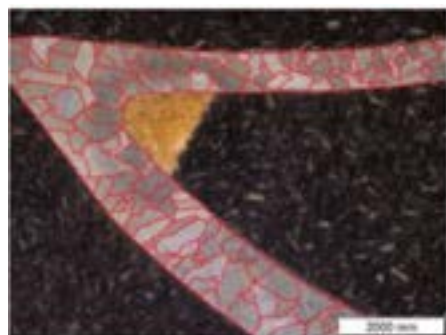
Grain size and shape was determined by means of a Cellular Automata model that assumed grain nucleation on the mould surface.

The nucleation rate was given by
$$\frac{dn}{d(\Delta T)} = \frac{n_{max}}{\sigma_{\Delta T} \cdot \sqrt{2\pi}} \exp\left[-\frac{1}{2}\left(\frac{\Delta T - \Delta T_m}{\sigma_{\Delta T}}\right)^2\right]$$
 where ΔT was the local undercooling and n_{max} , ΔT_m and $\sigma_{\Delta T}$ are the model parameters.

Grain orientation was random and grain growth was given by $v(\Delta T) = a\Delta T^2 + b\Delta T^3$

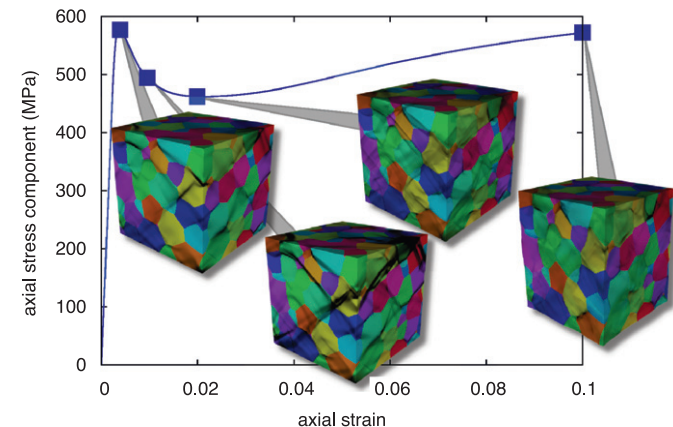


GRAIN SIZE in a GUIDE VANE



	Leading edge		Middlepart		Trailing edge	
	Exp.	Model	Exp.	Model	Exp.	Model
Grain size (μm)	1560	1345	785	869	281	397
Std. deviation	813	508	451	361	213	138
Aspect ratio	2.2	2.5	2.5	3.0	1.6	2.0

Virtual testing of polycrystalline materials can now be achieved by means of computational homogenization.



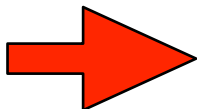
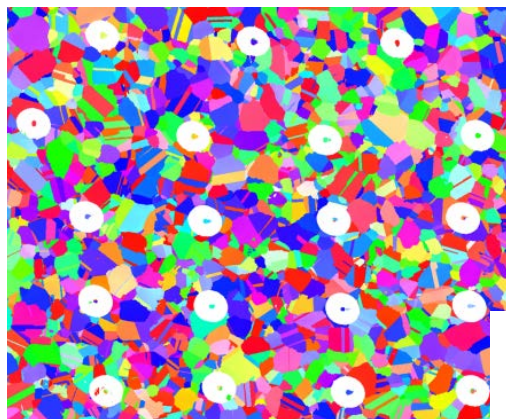
Key ingredients

Microstructural features: Grain size, shape and orientation distributions *easily* obtained by means of 2D and 3D characterization techniques (including serial sectioning, X-ray μ tomography, 3D EBSD, X-ray diffraction, etc.)

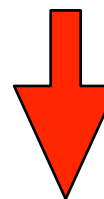
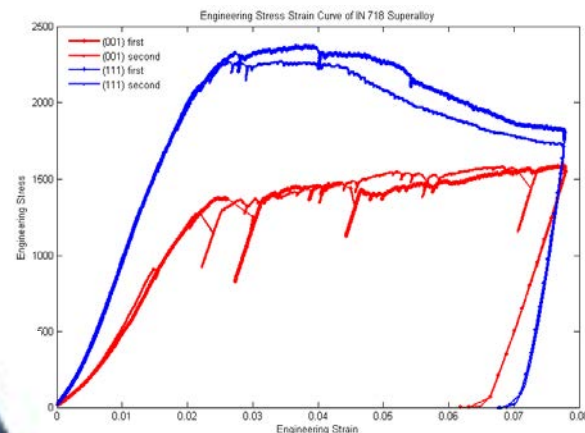
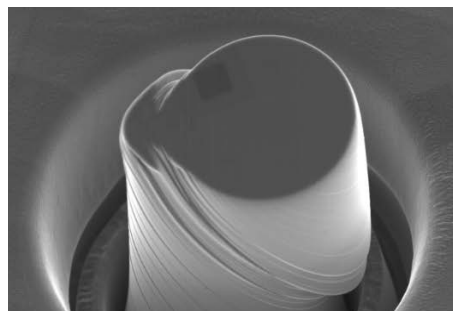
Single crystal behavior: CRSS for each slip system and twinning (including latent and forest hardening) provided by

- Multiscale modelling
- Mechanical tests of single crystals
- Inverse problem: back up single crystal behavior from tests on polycrystals
 - Homogenization of polycrystals
 - Nanoindentation

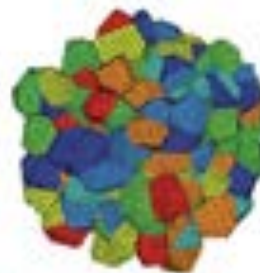
polycrystalline IN718



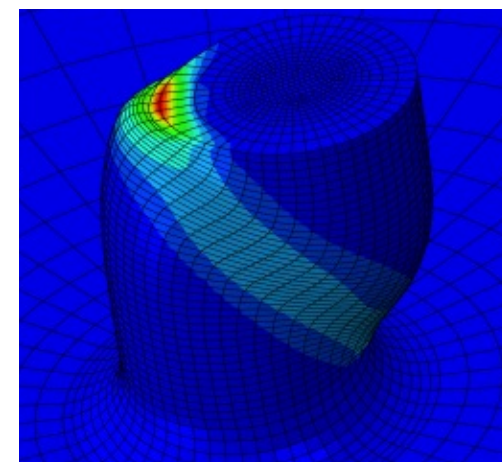
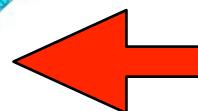
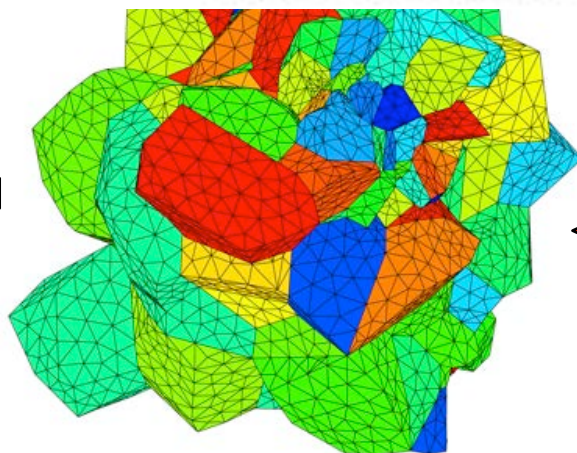
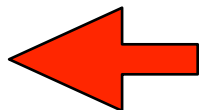
single crystal properties (T, strain rate) from micropillar tests



capsul
crystal plasticity simulation



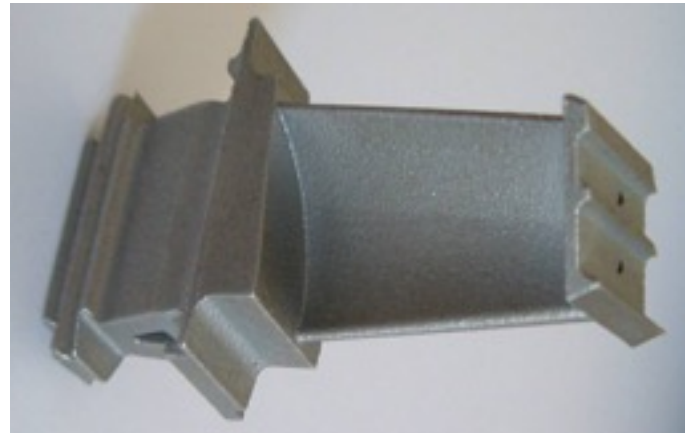
Macroscopic
mechanical
properties
(strength,
fatigue,
creep)



single crystal plasticity model

- Inconel 718 is a polycrystalline Ni-based superalloy used in cast or wrought form for high temperature structural applications up to 650-700°C.
- The most widely used Ni-based superalloy due to its good castability and weldability, high mechanical properties and corrosion resistance and low cost.

Turbine disk

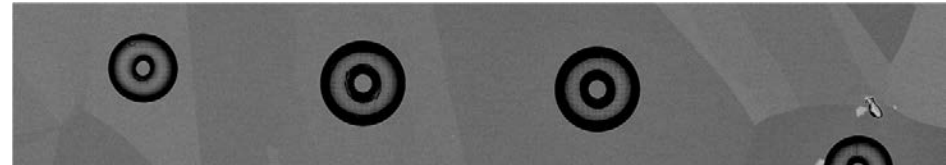
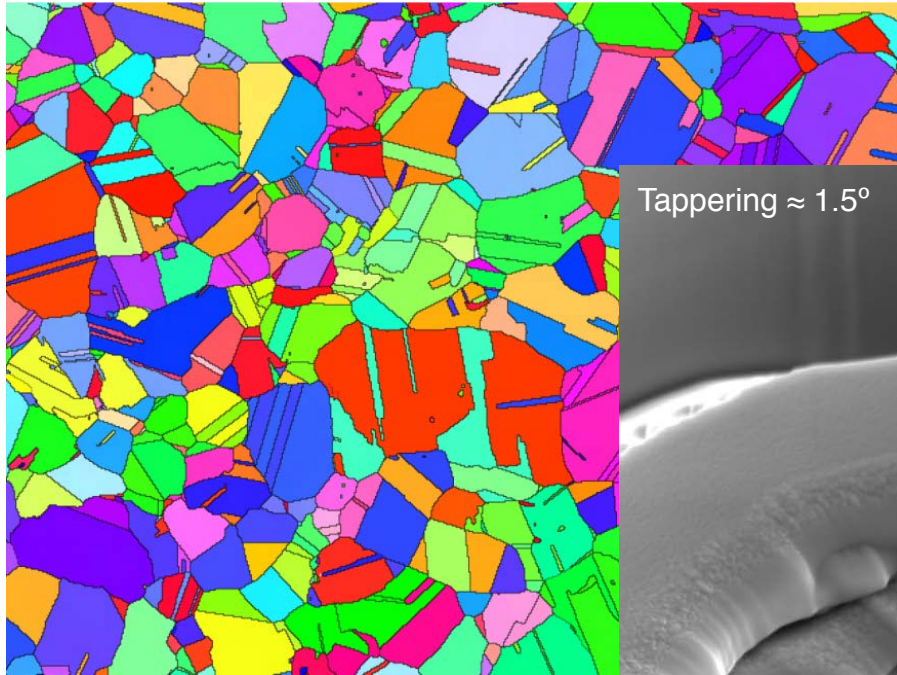


Turbine blade

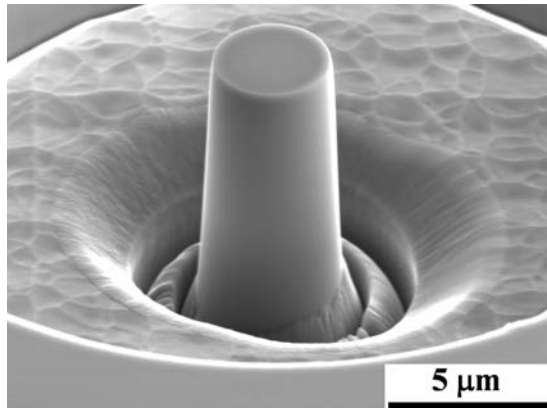
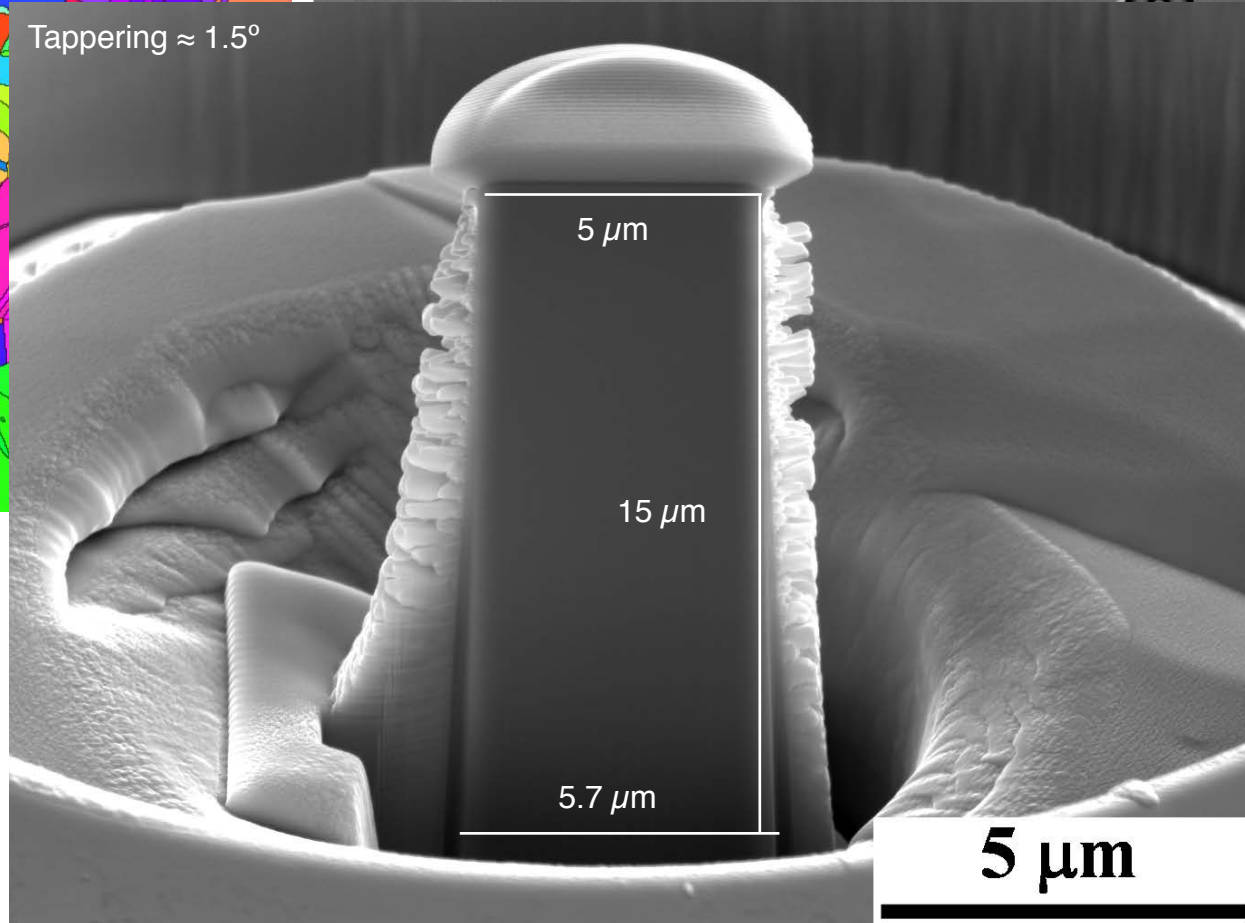
Chemical composition

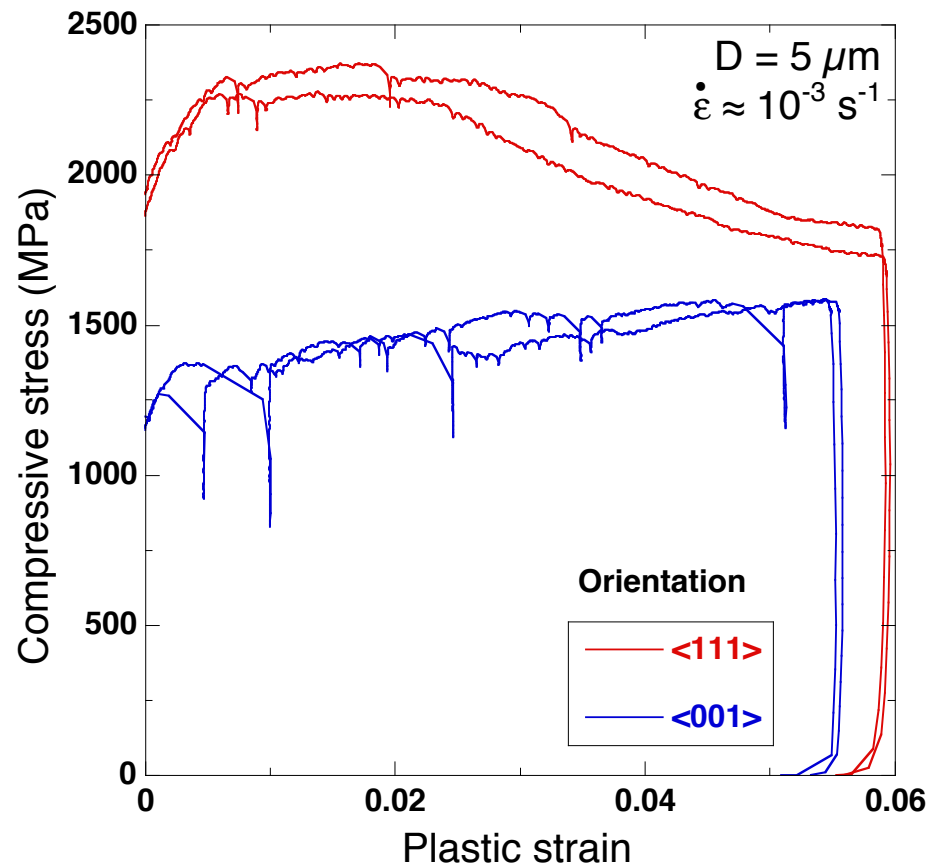
Element	Ni	Fe	Cr	Mo	Nb	Al	Ti	C
Weight (%)	balance	18.5	19.0	3.0	5.1	0.5	0.9	0.04

Single crystal properties as a function of orientation, temperature and strain rate were obtained by means of micropillar compression tests.



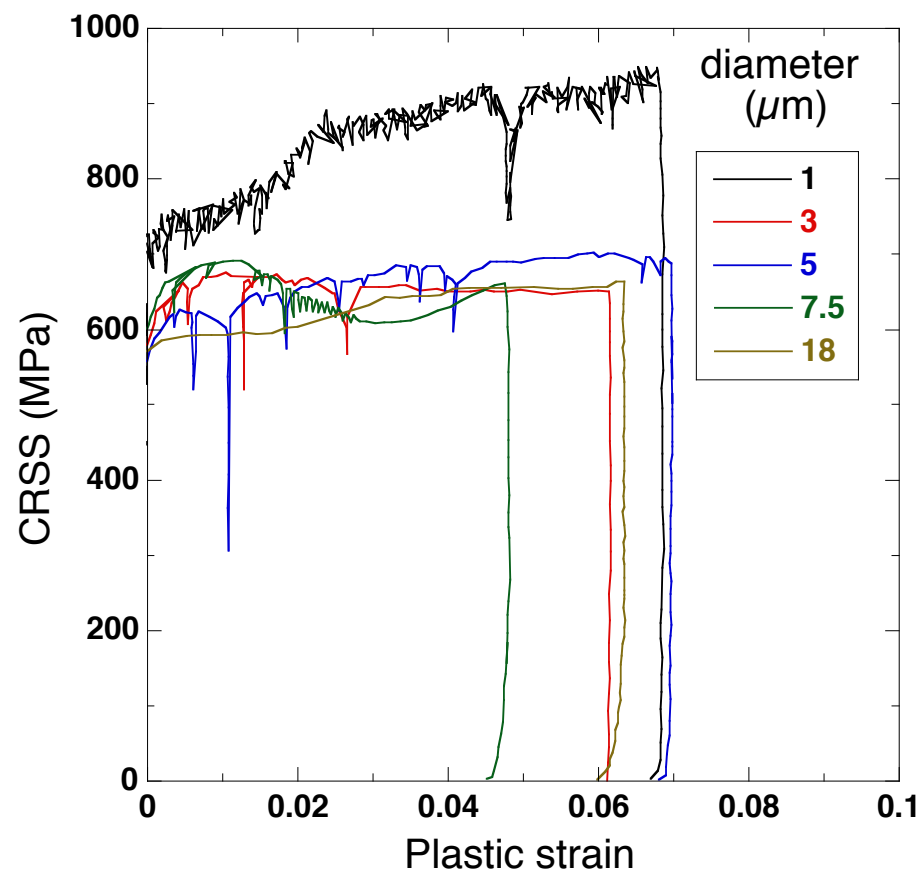
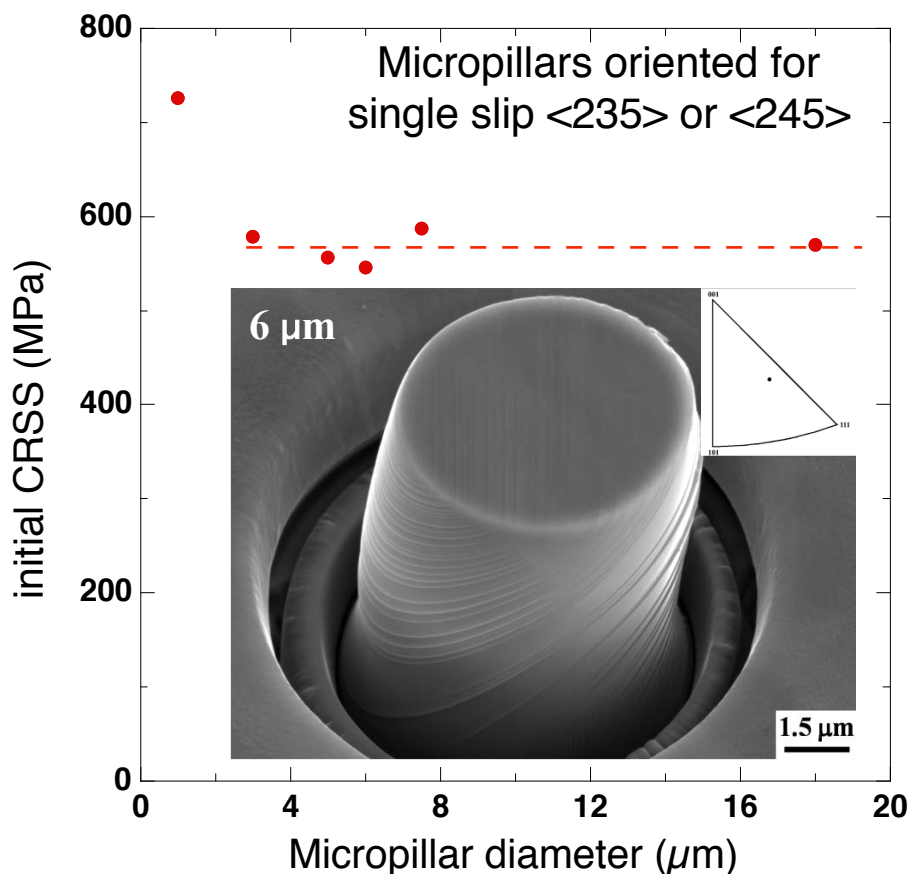
Tapering $\approx 1.5^\circ$







- Micropillar compression tests show limited experimental scatter.
- Partial unloadings were due to dislocation bursts.

Size effect



-  No size effects on the initial CRSS nor in the strain hardening were observed for micropillars with $D > 3 \mu\text{m}$.
-  This is very likely due to the fact that the strength is controlled by the small spacing between γ' and γ'' precipitates.

The CRSS were obtained by fitting the micropillar compression tests with numerical simulations carried out using a crystal plasticity finite element model.

- A crystal plasticity model was implemented as a UMAT in Abaqus/Standard
- Multiplicative decomposition $\mathbf{F} = \mathbf{F}^e \mathbf{F}^p$; velocity gradient $\mathbf{L} = \mathbf{L}^e + \mathbf{F}^e \mathbf{L}^p \mathbf{F}^{e^{-1}}$
- Plastic deformation in a FCC crystal is accommodated by N ($=12$) slips systems corresponding to the $\{111\}\langle 110 \rangle$ family:

$$\mathbf{L}^p = \sum_{\alpha=1}^N \dot{\gamma}^{\alpha} (\mathbf{s}^{\alpha} \otimes \mathbf{m}^{\alpha})$$

- The Green-Lagrange elastic strain is expressed as $\mathbf{E}^e = \frac{1}{2} (\mathbf{F}^{e^T} \mathbf{F}^e - \mathbf{I})$
- and the second Piola-Kirchoff stress tensor is given by

$$\mathbf{S} = \mathbb{C} \mathbf{E}^e = \mathbb{C} \left[\frac{1}{2} (\mathbf{F}^{e^T} \mathbf{F}^e - \mathbf{I}) \right]$$

where \mathbb{C} stands for the fourth-rank elastic stiffness tensor of the crystal.

🕒 The single crystal behaves as an elasto-viscoplastic solid:

- Shear strain rate in system α : $\dot{\gamma}^\alpha = \dot{\gamma}_0 \left| \frac{\tau^\alpha}{\tau_c^\alpha} \right|^{1/m} \text{sgn}(\tau^\alpha)$
- Resolved shear stress in system α : $\tau^\alpha = \mathbb{C} \left[\frac{1}{2} \left(\mathbf{F}^{eT} \mathbf{F}^e - \mathbf{I} \right) \right] : (\mathbf{s}^\alpha \otimes \mathbf{m}^\alpha)$



$$\tau^\alpha = \mathbf{S} : (\mathbf{s}^\alpha \otimes \mathbf{m}^\alpha)$$

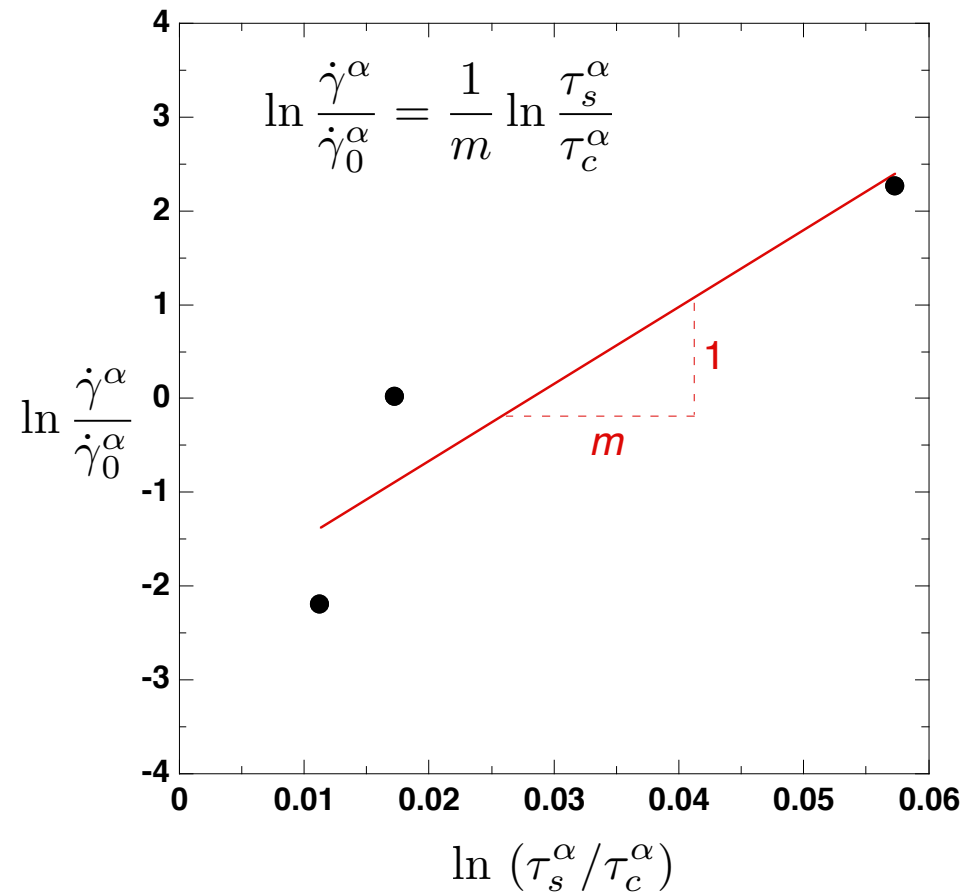
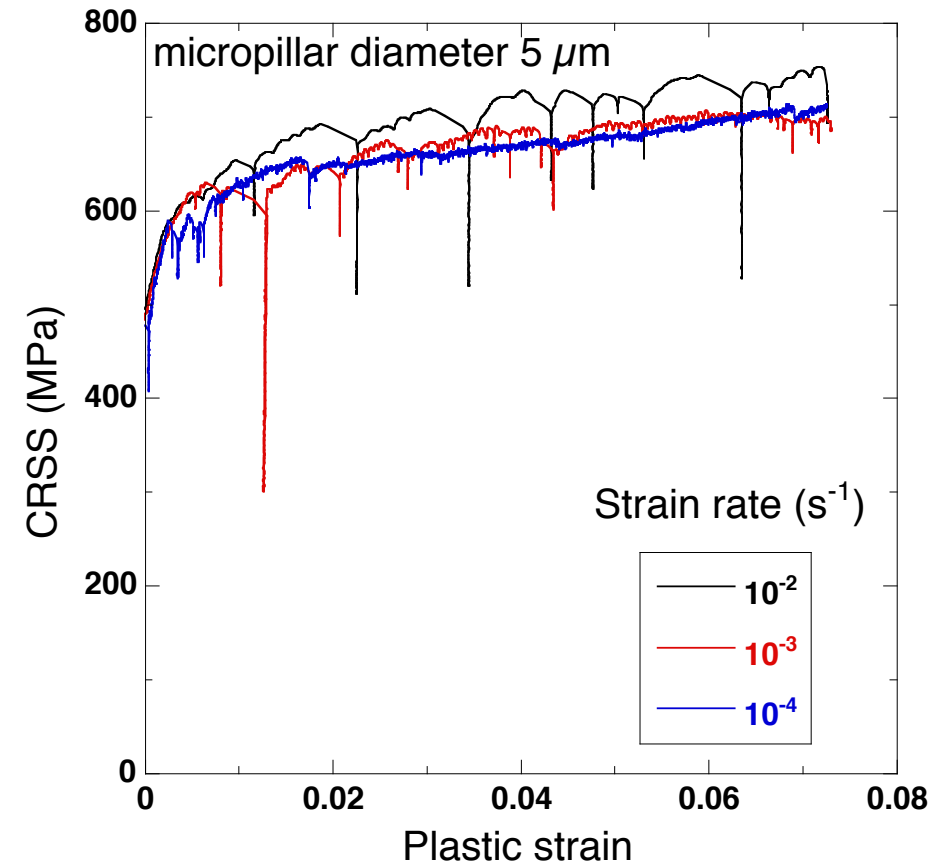
- Critical resolved shear stress in system α : $\tau_c^\alpha = \sum_{\beta} q_{\alpha\beta} h |\dot{\gamma}^\beta|$
- Hardening modulus h is given by the Voce Model:

$$h(\gamma) = h_s + (h_0 - h_s + \frac{h_0 h_s \gamma}{\tau_s - \tau_0}) \exp \frac{-\gamma h_0}{\tau_s - \tau_0} \quad \gamma = \int_0^t \sum_{\alpha} |\dot{\gamma}^\alpha| dt$$

🕒 The mechanical behavior of the single crystal is given by:

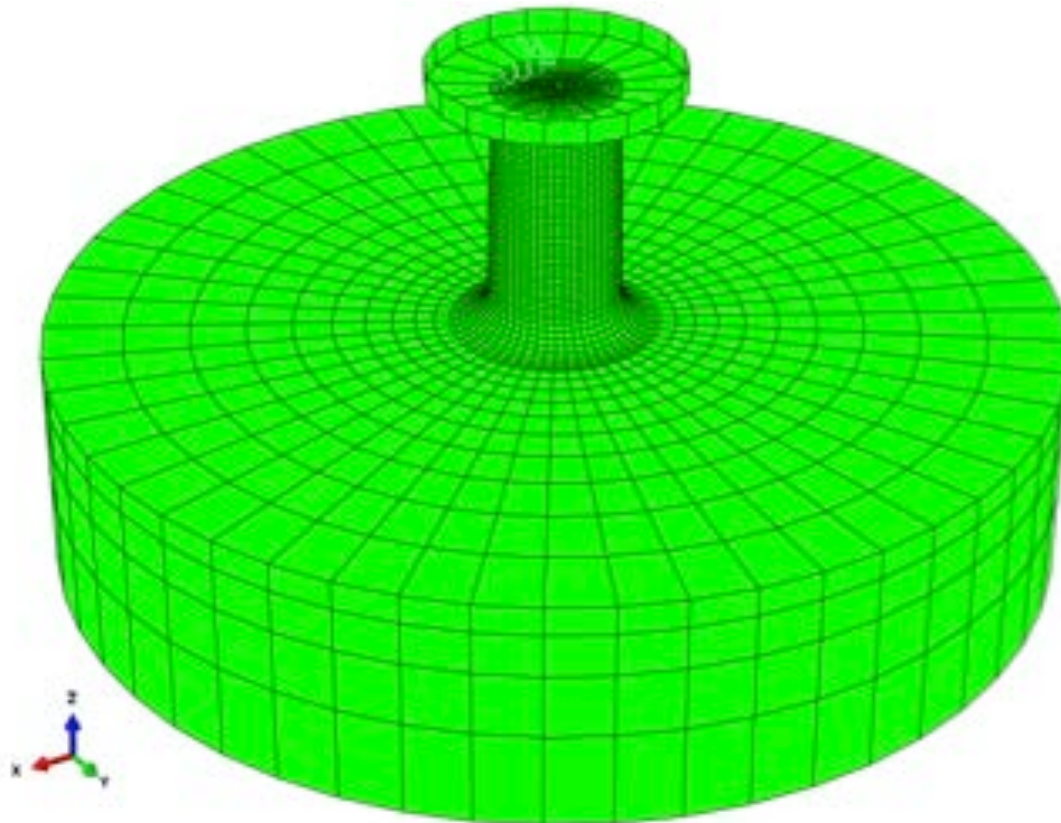
- \mathbb{C} : $C_{11} = 260$ GPa; $C_{12} = 179$ GPa; $C_{44} = 110$ GPa for IN718
- $\tau_0, \tau_s, h_0, h_s, q_{\alpha\beta}$ and the strain rate sensitivity m are obtained from micropillar compression tests.

Strain rate sensitivity $m = 0.017$



Limited strain rate sensitivity of IN718 at ambient temperature.

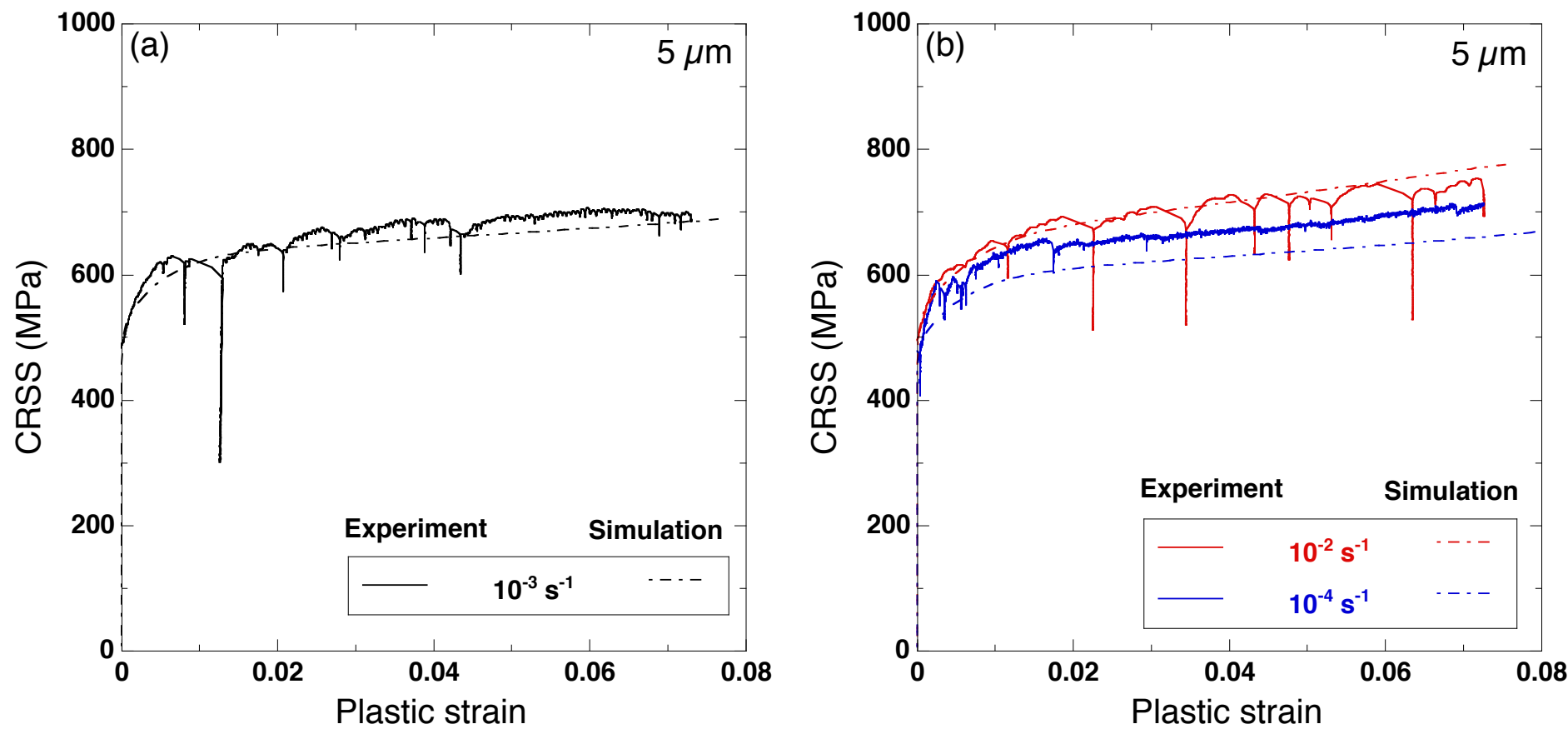
- Micropillar compression tests were simulated using the crystal plasticity model.
- The model includes the curvature at the fillet and the taper angle ($\approx 1.5^\circ$).
- The flat punch was modelled as rigid body with a lateral stiffness of $10 \mu\text{N/nm}$.
- Coulomb friction ($\mu = 0.1$) between flat punch and micropillar.
- Discretization with 8-noded liner brick elements (C3D8).



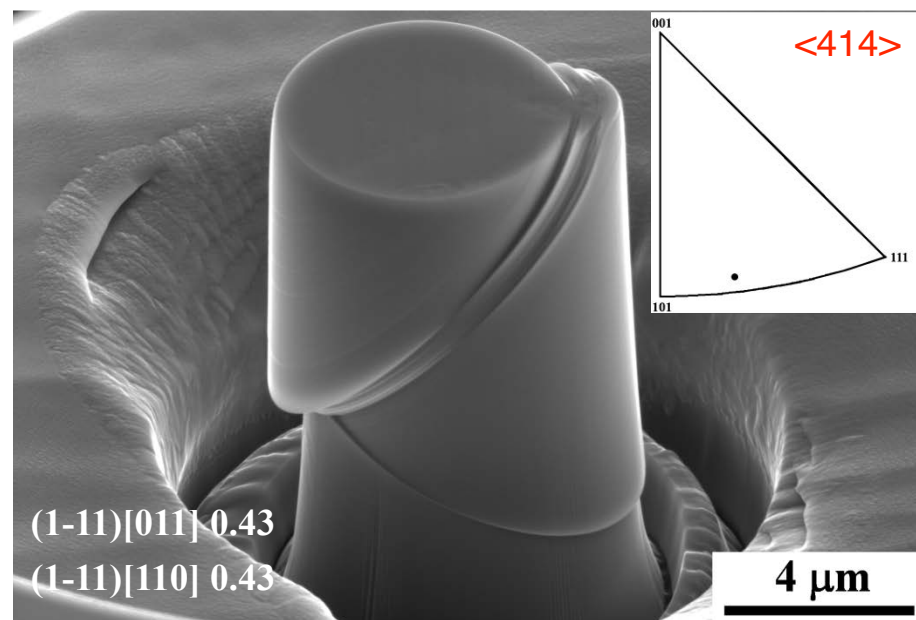
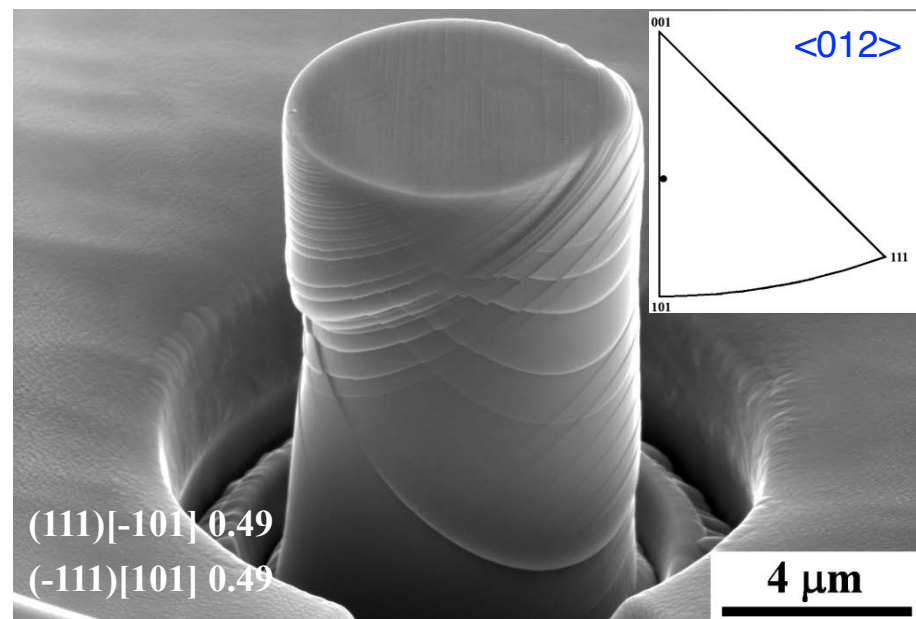
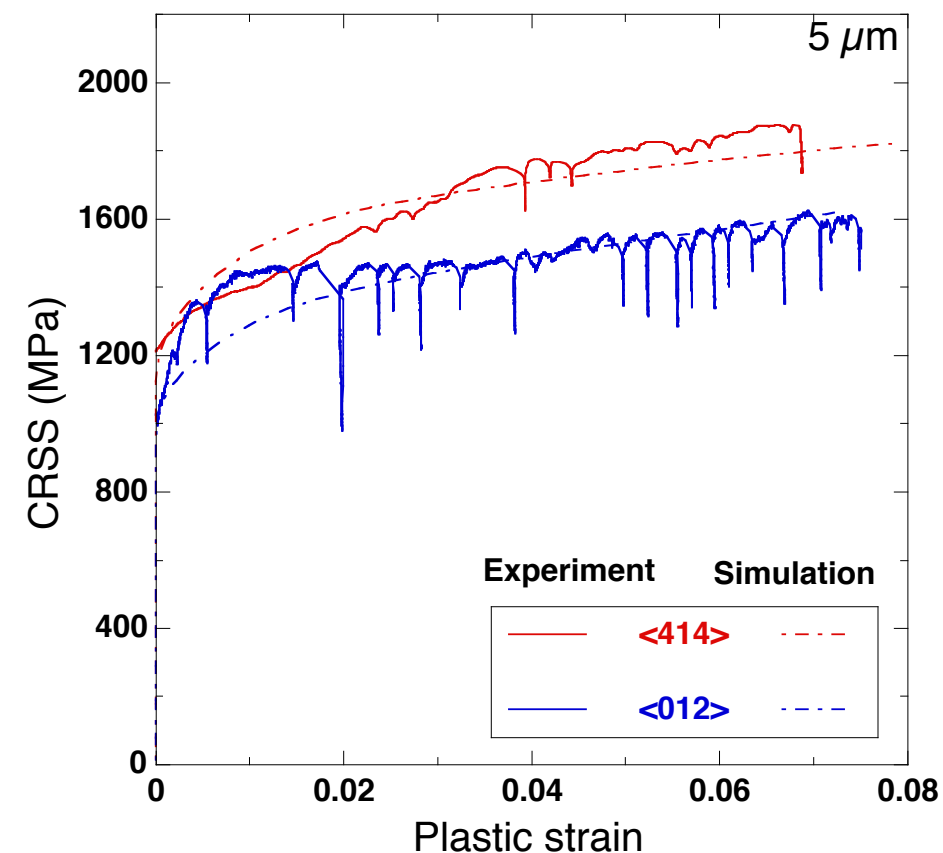
τ_0	τ_s	h_0	h_s	$q_{\alpha\beta}$
(MPa)	(MPa)	(GPa)	(GPa)	
466	599	6	0.3	1



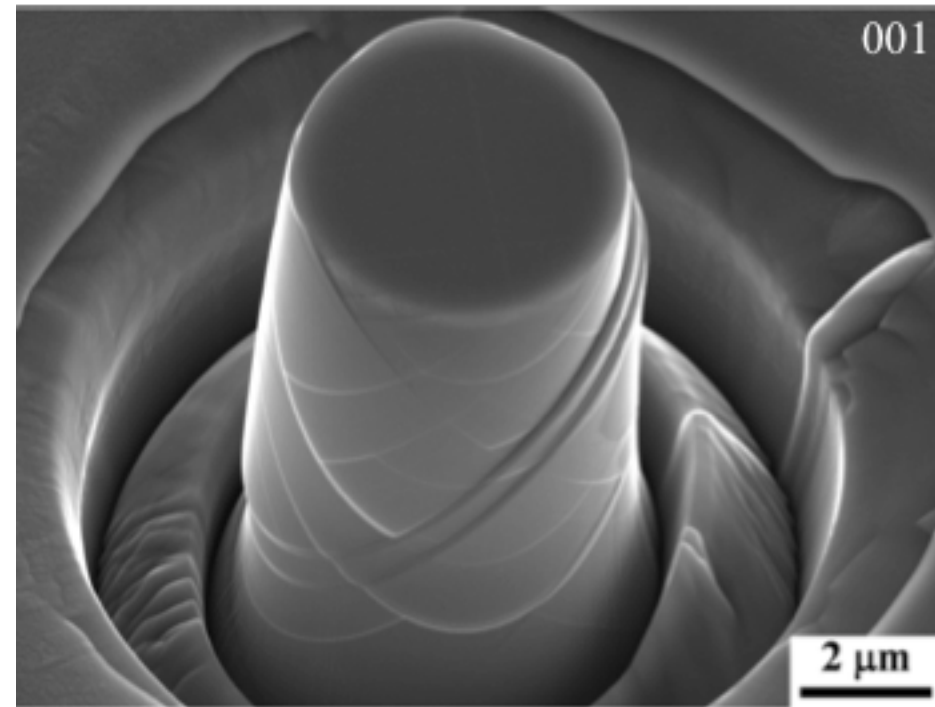
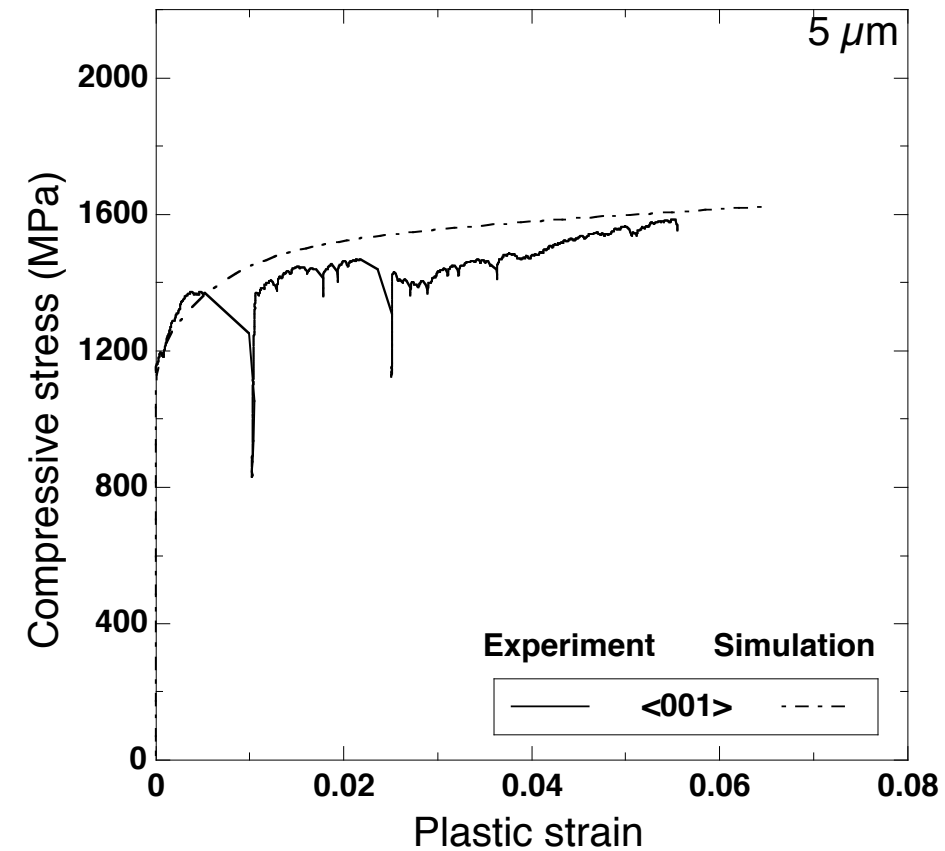
Effect of strain rate (single slip <123> and <235>)



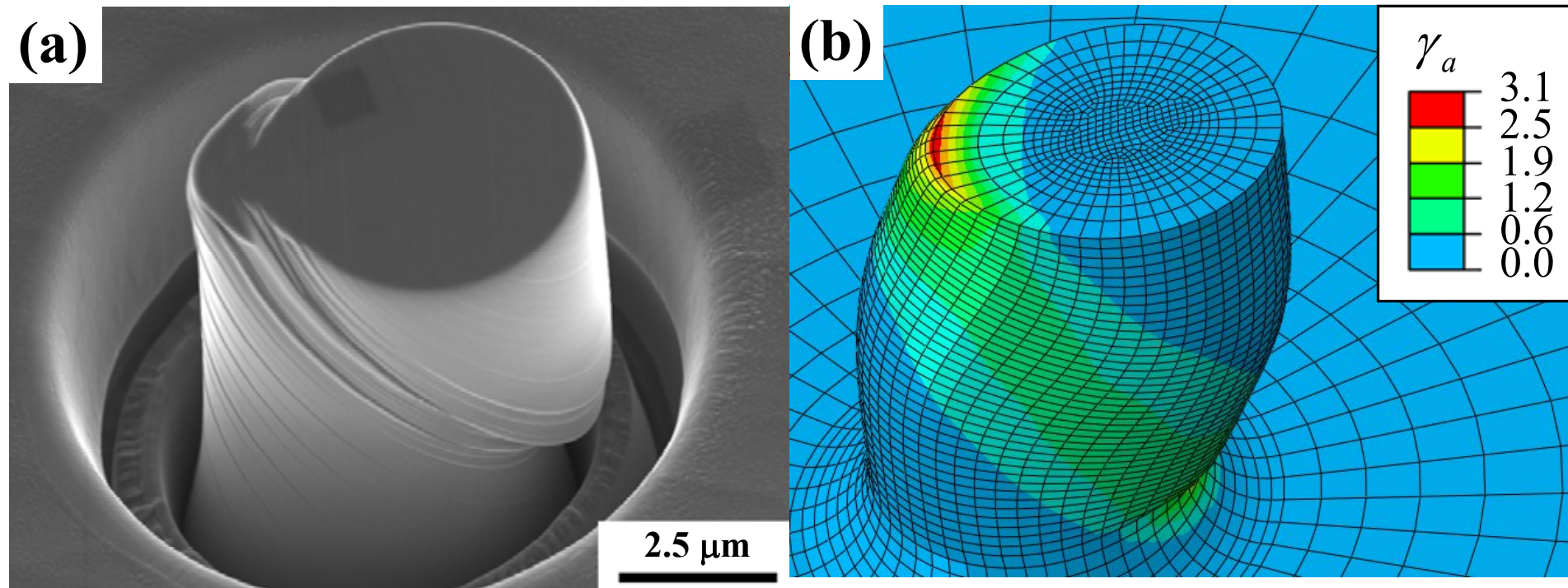
Effect of double slip: coplanar $\langle 414 \rangle$ and non coplanar $\langle 012 \rangle$




Multiple slip condition $\langle 001 \rangle$





Deformed micropillar along $\langle 212 \rangle$




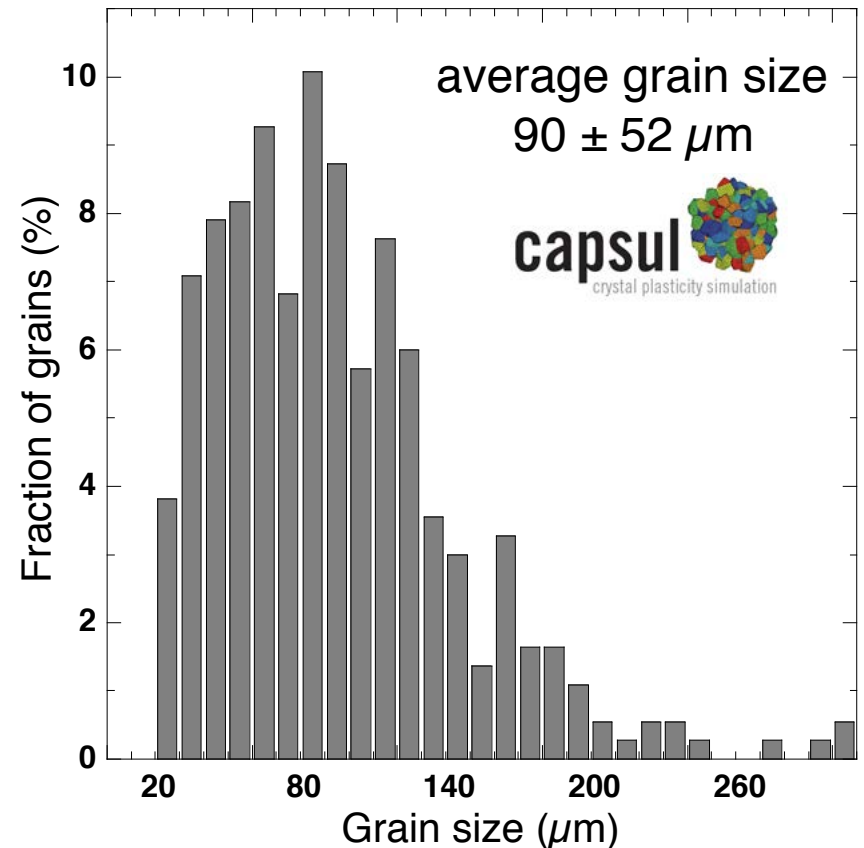
 The mechanical behavior of the polycrystal is computed by means of the finite element simulation of the mechanical behavior of a representative volume element of the microstructure with periodic boundary conditions.

Representative Volume Element

 2D grain size distribution obtained from micrographs is transformed into 3D using **strip-star** (Basel University).

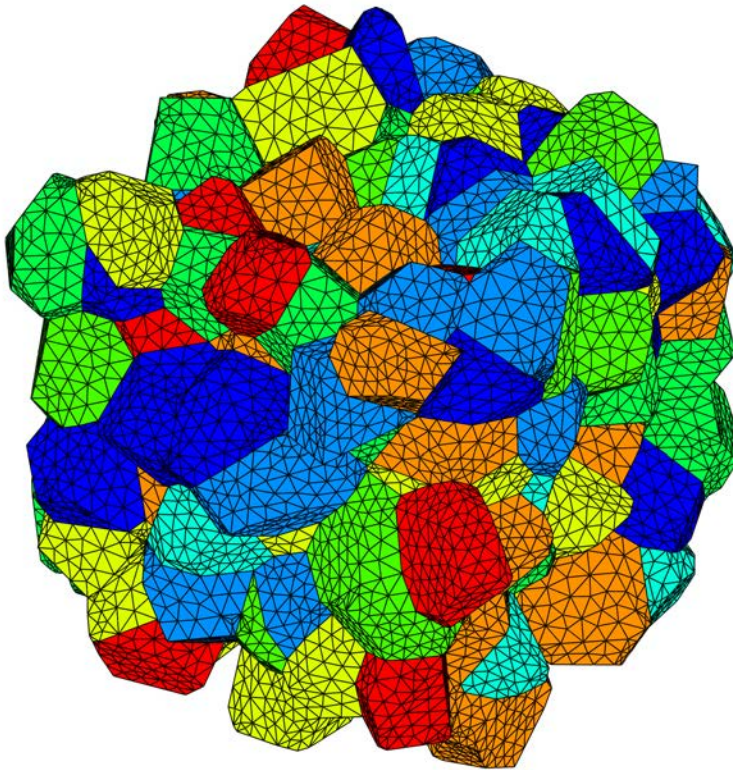
 RVE is obtained by the Laguerre tessellation of an initial set of points obtained from a Monte Carlo algorithm to provide the actual grain size distribution 3D

 The orientation of the grains within the RVE was random.



finite element model

- Discretization was carried out 10-noded quadratic tetrahedral elements (C3D10).
- Sensitivity analysis: number of grains in RVE and number of elements per grain

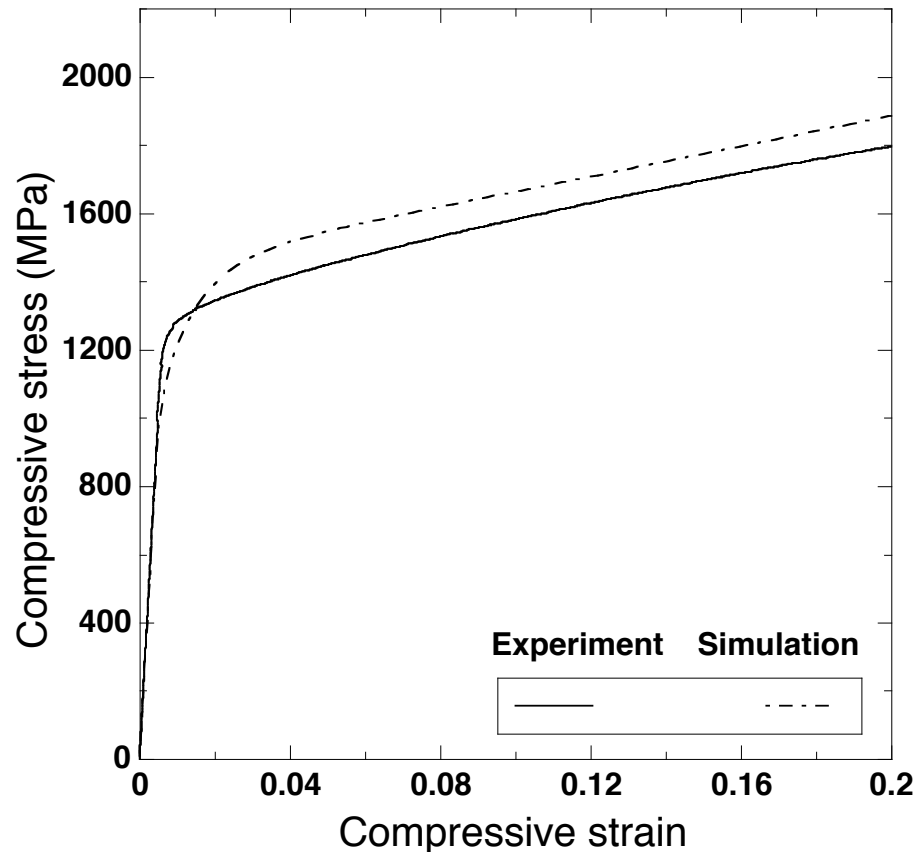


210 grains
 610 finite element per grain

Periodic boundary conditions

- The displacement of opposite pairs of nodes on the RVE surfaces $\mathbf{x}_B - \mathbf{x}_A = \mathbf{L}_{AB}$ is given by $\mathbf{u}_B - \mathbf{u}_A = (\bar{\mathbf{F}} - \mathbf{I}) \mathbf{L}_{AB}$ where $\mathbf{L}_{AB} = (L, 0, 0), (0, L, 0)$ or $(0, 0, L)$

Uniaxial compression of polycrystalline IN718 at 25°C and $5.0 \cdot 10^{-4} \text{ s}^{-1}$



- Good agreement between experiments and simulations: validation of the strategy.
- Opens the way for further developments: high temperature, fatigue, creep, etc...

CONCLUSIONS

- Virtual design, virtual processing and virtual testing of engineering alloys is becoming feasible by means of multiscale, bottom-up approaches.
- Current available approaches still have to rely in phenomenological models (cellular automata model of grain nucleation and growth) and experiments (micropillar compression) provide accurate predictions for engineering alloys components. That will be gradually replaced by rigorous models based on ab initio and atomistic simulations as well as by more sophisticated coupling between simulations tools (phase field - computational thermodynamics - computational kinetics).

ACKNOWLEDGEMENTS

- Dr. J. Segurado, IMDEA Materials Institute & Polytechnic University of Madrid
- Dr. J. M. Molina-Aldareguía, IMDEA Materials Institute
- Dr. I. Sabirov, IMDEA Materials Institute
- Dr. M. Rahimian, Dr. A. Cruzado & Dr. B. Gan, IMDEA Materials Institute
- Mr. M. Jiménez, IMDEA Materials Institute

ACKNOWLEDGEMENTS




VANCAST project (*Next Generation Nozzle Guide Vanes*), EU 7th FP, ERA-NET Matera+.




MICROMECH project (*Microstructure-based Material Mechanical Models for Superalloys*), EU 7th FP, Clean Sky JTI, grant agreement n° 62007




VIRMETAL project (*Virtual Design, Virtual Processing and Virtual Testing of Metallic Materials*), ERC Advanced Grant, EU H2020 programme, grant agreement n° 669141